Proceedings of the
International Conference on Mechanical Engineering 2005
(ICME2005) 28- 30 December 2005, Dhaka, Bangladesh

ICME05-TH-40

AN ANALYTICAL STUDY ON CRITICAL HEAT FLUX DURING NATURAL CONVECTIVE BOILING IN A VERTICAL TUBE

M A Islam[1*], H M M Afroz[1] and M Monde[2]

[1]Department of Mechanical Engineering, BUET, Dhaka-1000, Bangladesh.
* aislam@me.buet.ac.bd
[2]Department of Mechanical Engineering, Saga University, 1 Honjo-machi, Saga 849-8502, Japan.

ABSTRACT

An analytical study is performed for the prediction of Critical Heat Flux (CHF) during natural convective boiling in a vertical uniformly heated tube, submerged in a saturated liquid bath, by a model where vapor forms a paraboloid under co-current flow situation. Mass, momentum and energy balances for the two-phase flow in the vertical tube are used to construct the model together with the criterion that the CHF is considered to be taken place at the exit of the heated tube when mass flux is maximum. Using this model, about 300 CHF data are predicted for saturated Water, R113 and R12 at different pressures for different tube geometries. The characteristics of CHF predicted are explained and compared with similar existing experimental results.

Keywords: Critical Heat Flux, Analytical Study on CHF, Natural Convective Boiling.

1. INTRODUCTION

Critical Heat Flux (CHF) during natural convective boiling in a vertical tube is triggered when liquid in contact with heated wall disappears due to continuous evaporation and consequently the heated wall is exposed to vapor. In this case heat transfer from the heated wall is suddenly deteriorated and the wall temperature increases rapidly, which may cause significant damage to a system. Thus the prediction of CHF is a prior design consideration regarding safety and economic optimization of various industrial heat transfer equipments such as superconductive devices, microelectronic devices, nuclear reactor core, evaporator in a refrigeration or air conditioning unit and boiler of conventional and nuclear power plant etc.

In the present days, enormous data and various empirical, semi-empirical correlations for CHF are available for each application. However, the applicable range of those correlations is geometrically and thermal-hydraulically confined to the experimental conditions. The parametric trends are, however, identified from the data collected so far. A comprehensive theoretical model or correlation is yet to be developed so that it can be applied universally to predict CHF for various fluids at various thermal-hydraulic and geometric conditions.

Katto [1] developed a generalized correlation for the CHF during natural convective boiling in confined channels with the aid of dimensional analysis. In 1979, Katto and Kurosaka [2] measured the CHF for three liquids (Water, Ethanol, and R113) except for cryogenic liquids and annular channels. They explained three characteristics CHF regimes and developed generalized correlations for two of the regimes. Monde and Yamaji [3] measured CHF during the natural convective boiling in a vertical uniformly heated tube submerged into a saturated liquid. They used Water, R113 and R12 as working fluids and proposed two generalized correlations to predict CHF for two characteristics regimes. Monde et al. [4] made an analytical study of the critical heat flux of a two phase thermosyphon, in which liquid and vapor form a countercurrent annular flow. They derived two correlations for two limiting conditions. Katto and Yokoya [5] proposed a preliminary model describing the macrolayer dryout as the mechanism leading to CHF in pool boiling. Later, Haramura and Katto [6] completed the model development by introducing the mechanism for macrolayer formation in both pool and flow boiling.

CHF in annular film flow regime can be determined at the point where the processes of evaporation, deposition, and entrainment lead to a condition in which the film flow rate becomes zero. Analytical treatments of this type have been explored in depth by Whalley, Hewitt, and co-workers [7-10]. The results of these investigations indicate that this type of method can be used successfully to predict CHF conditions for forced-convective boiling in tubes, annuli, and rod bundles. Okawa et al. [11] predicted CHF in annular flow using a film flow model. Their predicted results agree with the experimental data fairly well when the flow pattern at the onset of critical heat flux condition is considered annular flow.

From the above discussion it is clear that a very few

analytical studies on CHF of natural convective boiling have been carried out to obtain the fundamental design information necessary to apply the system as an efficient heat transfer device. Thus the present study is devoted to develop an analytical method to predict the CHF during natural convective boiling in vertical heated tubes submerged in a saturated liquid bath where vapor and liquid constitute a co-current flow.

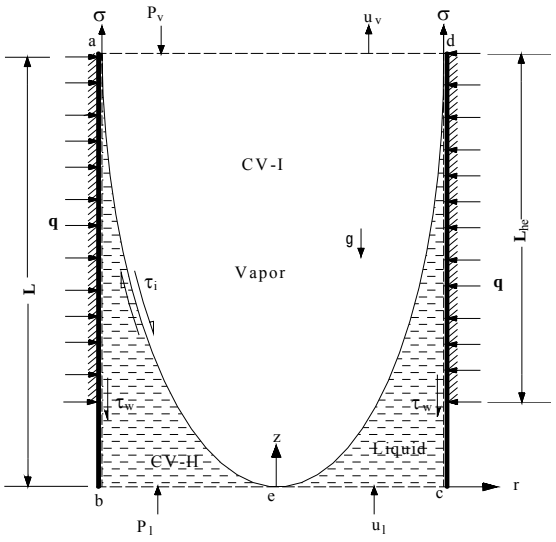

Fig 1. Idealized flow model for CHF analysis where $L <$ or $\geq L_{he}$

2. ANALYSIS METHODOLOGY

2.1 Model

Under co-current flow situation shown in Fig.1, the vapor forms a paraboloid formed by Eq.(1), where the exponent *n* is the profile index.

$$\frac{z}{L}=\left(\frac{r}{r_o}\right)^n \qquad \text{for } n\geq 2 \tag{1}$$

Where r and z are, respectively, the coordinates in horizontal and vertical directions and r_0 is the radius of the heated tube. The profile length, L may vary in such a way that it may be greater than, less than or equal to the tube heating length, L_{he}. The CHF is assumed to be taken place at the exit of the heated tube when the void fraction is unity. In addition to this assumption, both entrainment and deposition of liquid are ignored and the two phases are considered in local thermodynamic equilibrium and the flow is considered steady even though two-phase flow in the tube was oscillating as mentioned in the study by Monde et al [3].

According to the Fig.1 the mass conservation for the control volume I containing vapor and control volume II containing liquid is given by Eq. (2).

$$\int_{CSI}\rho u dA = \int_{CSII}\rho u dA = 0 \tag{2}$$

The momentum balance of the control volume (I) in the z-direction can be expressed as-

$$-\int_{CVI}\rho_v g dV + \int_{CSI} P dA - 2\pi\int_0^L r(\tau_i)_I dz$$
$$= \int_{CSI}(Gu)_{out}dA - \int_{CSI}(Gu)_{in}dA \tag{3}$$

And the momentum balance of the control volume (II), in the z direction is –

$$-\int_{CVII}\rho_l g dV + \int_{CSII} P dA + 2\pi\int_0^L r(\tau_i)_{II} dz - \int_0^L 2\pi r_0\tau_w dz$$
$$= \int_{CSII}(Gu)_{out}dA - \int_{CSII}(Gu)_{in}dA \tag{4}$$

For steady flow, the interfacial shear forces must be balanced. Adding Eq. (3) and Eq. (4) the following relation for the overall momentum balance of the control volume abcd can be obtained.

$$F_P - F_G - F_W - F_M = 0 \tag{5}$$

Where,

$F_P = \int_{CSI} P dA + \int_{CSII} P dA$ = Pressure Force

$F_G = g\left[\int_{CVI}\rho_v dV + \int_{CVII}\rho_l dV\right]$ = Gravity Force

$F_M = \int_{CSI}(Gu)_{out}dA - \int_{CSII}(Gu)_{in}dA$

= Rate of change of momentum

$F_W = \int_0^L 2\pi r_0\tau_w dz$ = Wall friction force

Through proper mathematical manipulation and suitable inlet velocity profile considerations [12], the above forces can be simplified as follows:

$$F_P = 2\pi r_0\sigma + \rho_l g\pi r_0^2 L \tag{6}$$

$$F_G = \pi r_0^2 gL\left[(\rho_v-\rho_l)\frac{n}{n+2}+\rho_l\right] \tag{7}$$

$$F_M = r_0^2 G^2\left(\frac{k_v}{\rho_v}-\frac{k_l}{\rho_l}\right) \tag{8}$$

$$F_W = \frac{\pi r_0^2 G^2 L}{\rho_l} I \tag{9}$$

Here, $I = \left[\int_0^{1-L^+}\frac{C_{fw}}{\left\{1-(z^+)^{2/n}\right\}^4}dz^+\right] +$

$$\left[\int_{1-L^+}^{1}\frac{C_{fw}(1-z^+)^2}{\left\{1-(1-L^+)^{2/n}\right\}^2 L^{+2}\left\{1-(z^+)^{2/n}\right\}}dz^+\right] \quad \text{for } L^+<1$$

$$= \int_0^1 C_{fw}\frac{(1-z^+)^2}{[1-(z^+)^{2/n}]^2}dz^+, \qquad \text{for } L^+=1$$

$$= \int_0^1 C_{fw}\frac{(1-z^+)^2}{L^{+2}[1-(z^+)^{2/n}]^2}dz^+, \qquad \text{for } L^+>1$$

And C_{fw}, the wall friction factor, can be obtained from the equations provided by Wallis [13] in the laminar and turbulent flow regions and by Monde [14] in the transition regions as follows:

$$C_{fw} = 16/Re_l \qquad \text{when } Re_l \leq 160 \tag{10}$$

$$C_{fw} = \mathrm{Exp}\begin{bmatrix} 5.48616 - 2.10284\log_e(\mathrm{Re}_l) + \\ 0.11855(\log_e \mathrm{Re}_l)^2 - 1.30035\times10^{-3}(\log_e \mathrm{Re}_l)^3 \end{bmatrix} \quad \text{when } 160 < \mathrm{Re}_l \le 10^4 \qquad (11)$$

$$C_{fw} = 0.079\,\mathrm{Re}_l^{-0.25} \qquad \text{when } \mathrm{Re}_l \ge 10^4 \qquad (12)$$

From the Eqs. (5-9), final form of the momentum equation becomes:

$$F_1(G,L) = \frac{\pi r_o G^2 L}{\rho_l} I + \left(\frac{k_v}{\rho_v} - \frac{k_l}{\rho_l}\right) r_0^{\,2} G^2 + \pi r_o^{\,2} g L(\rho_v - \rho_l)\frac{n}{n+2} + 2\pi r_0 \sigma = 0 \qquad (13)$$

At the CHF, q fixes the profile length, L maximizing the mass flux, G. Therefore, for maximum G, $\partial G / \partial L = 0$. In other words, the maximum condition can be expressed using Euler's theorem as given in Eq. (14)

$$\frac{\partial F_1}{\partial L} = 0 = F_2(G,L) \qquad (14)$$

This can again be rearranged as follows.

$$F_2(G,L) = \frac{\pi r_o G^2}{\rho_l}\left(L\frac{\partial I}{\partial L} + I\right) + \pi r_o^{\,2} g(\rho_v - \rho_l)\frac{n}{n+2} = 0 \qquad (15)$$

Solution of the simultaneous Eq.(13) and Eq.(15) will give the maximum G and then by using the energy balance, the value of CHF can be predicted by the following relation.

$$q_{co} = \frac{H_{lg} D G_{max}}{4 L_{he}} \qquad (16)$$

2.2 Solution Procedure

Knowing the properties of fluid and geometric parameters of the tube, one can solve the model follows:

(i) An initial guess is made for the mass flux, G and the profile length, L.
(ii) Within the guess range of G and L, the value of the functions $F_1(G,L)$ and $F_2(G,L)$ from the Eq. (13) and Eq. (15) are computed for a particular tube geometry, working fluid and working condition.
(iii) The contour of the functions $F_1(G,L)$ and $F_2(G,L)$ are plotted
(iv) The intersection point of the contour $F_1(G,L) = 0$ and $F_2(G,L) = 0$ is the solution of the Eq.(13) and Eq.(15) and gives the maximum mass flux, G_{max} for a particular tube geometry and thermal-hydraulic condition of the working fluid.
(v) The value of G_{max} is used to calculate q_{co} using the Eq. (16).

3. RESULTS AND DISCUSSIONS

Using the model described above, about 300 CHF data have been predicted by varying the tube geometry and thermal-hydraulic conditions of the various working fluids, with a view to evaluating the effects of various parameters on CHF, making comparison and evaluating performance of the model.

3.1 Effects of Interface Profile Shape

It has been found that profile shape has significant influence on the CHF of present boiling system. Fig. 2 shows the variation of CHF with the profile index 'n' for the working fluid R113 at a fixed L_{he}/D. It shows that with the increase of 'n' the CHF decreases because the void fraction increases with 'n'. The change of the CHF is significant upto 'n' = 8 for R113 and then further increase of 'n' has very little effect on CHF. For other fluids, significant values of 'n' are yet to be found out. For these reason, n=3 has been used to calculate the CHF for the present conditions.

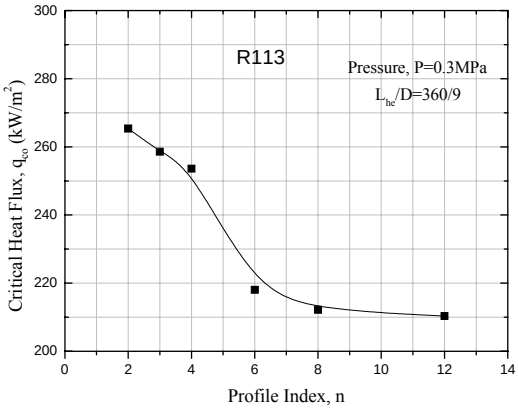

Fig 2. Effect of profile index on q_{c0}

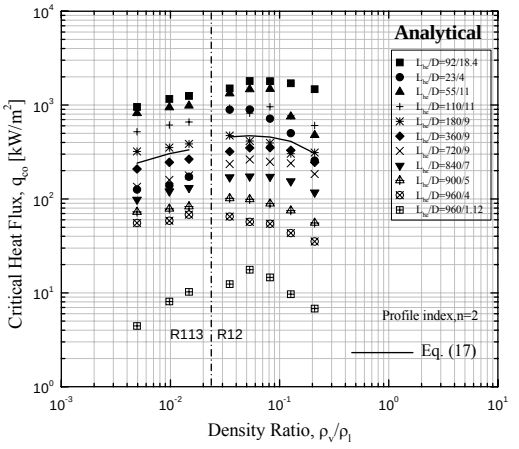

Fig 3. CHF characteristics

3.2 CHF Characteristics

Figure 3 has been constructed with the present analytical data to explain the basic CHF characteristics of R113 and R12, and Fig.4 representing the experimental data [3] has been constructed to compare the characteristics of CHF with the analytical ones. Figure 3 represents all the CHF data plotted against the density

ratio (ρ_v/ρ_l). The solid line for each working fluid as shown in this figure is the Kutateladze correlation (17) for predicting the CHF in an ordinary saturated pool boiling.

$$Ku = \frac{q_{co}/\rho_v H_{lg}}{\sqrt[4]{\sigma g(\rho_l - \rho_v)/\rho_v{}^2}} = 0.16 \qquad (17)$$

Each of the symbols in Fig. 3 represents a CHF data for a particular combination of heating length and diameter of the tube. The CHF in a vertical tube basically depends on the ratio L_{he}/D and ρ_v/ρ_l and its character has a tendency similar to Kutateladze's prediction for saturated pool boiling. The CHF of the present analysis should be smaller than the Kutateladze's prediction (17) because this analysis is done for the boiling in a narrow confine of a tube whereas Eq. (17) is for pool boiling. But the Fig. 3 shows that some of the CHF for smaller L_{he}/D are higher than the Kutateladze's prediction. This may be due to lower value of 'n' and the various assumptions that are considered for the simplification of this analysis. We hope that higher values of 'n' will certainly improve the CHF prediction by this model.

For the same value of L_{he}/D, the CHF increases with an increase of ρ_v/ρ_l for R113, while decreases for R12. This is because of the working pressures chosen in this study such that the reduced pressure, P_r, is in the range of 0.192 to 0.703 for R12 and $P_r << 0.192$ for R113. It is well known that the CHF increases with P_r and becomes maximum at a working pressure of about $P_c/3$ (i.e. $P_r=1/3$), beyond which it decreases continuously [13]. As P_r increases with ρ_v/ρ_l, the CHF as shown in Fig. 3 is obtained. It is worth mentioning that for a constant ρ_v/ρ_l, the CHF increases with an increase in tube diameter for a fixed length of the tube and decreases with an increase in tube length for a constant tube diameter. These are also explained clearly later.

The Characteristics of the analytical CHF values in the Fig.3 shows the similar tendency as in the Fig.4, which shows the same of experimental values by Monde et al. [3]. The analytical model always over predicts the CHF compared to experimental values except those for the L_{he}/D=23/4 and L_{he}/D=960/1.12 for R113 and for L_{he}/D=960/1.12 for R12. Again for Water the analytical model under predicts the CHF for L_{he}/D = 960/4.

3.3 Effects of Tube Geometry

Influences of tube heating length and diameter ratio, L_{he}/D on CHF are shown in Fig. 4(a-c) where different symbols are for different working pressures. The solid line in the above figures is the Kutateladze correlation (17) drawn for easy comprehension of the CHF data. For all the working fluids, the CHF decreases with increase in L_{he}/D and the changes are more significant for L_{he}/D < 50 where 10 folds increase in L_{he}/D makes a decrease in the CHF of 20% while beyond this range the decrease is only 4%.

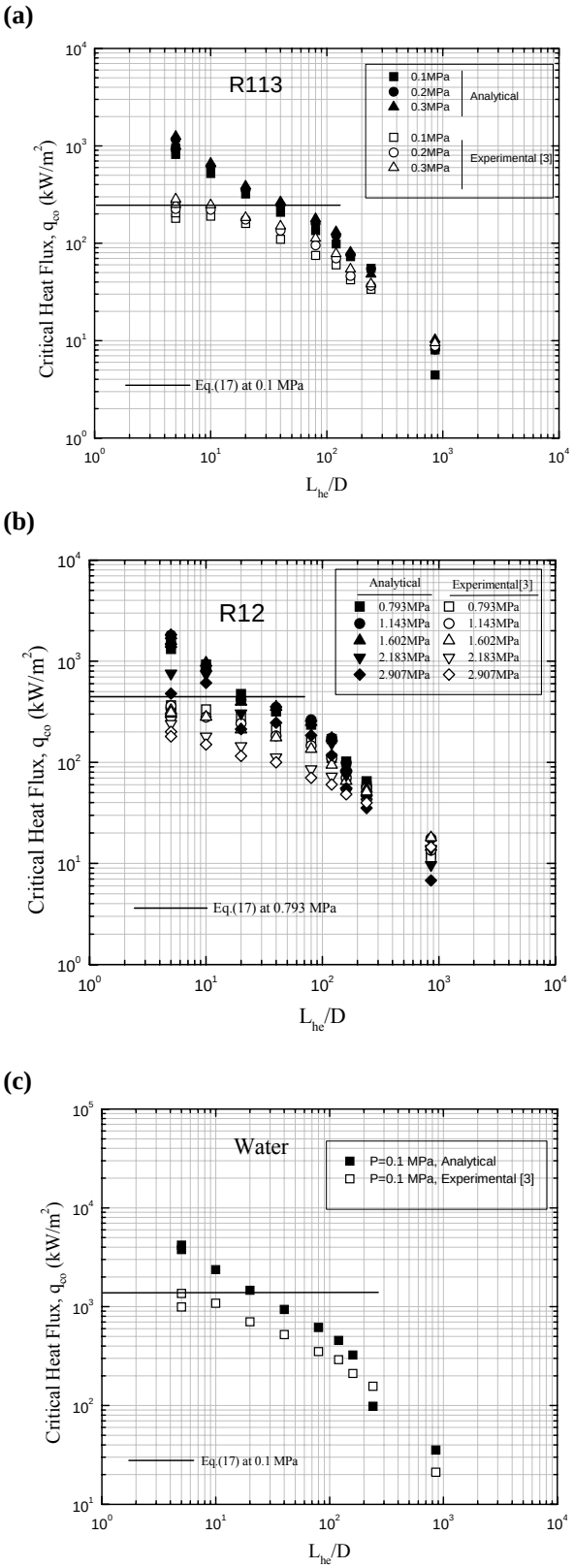

Fig 4. Effect of L_{he}/D on CHF for different liquids

3.4 Performance of the Model

In order to test the efficacy of the present analytical model, the CHF data for R113, R12 and water have been compared with the experimental data that were measured by Monde et al. [3] for similar geometry and thermal-hydraulic conditions. Fig. 5(a-c) shows the comparison of reciprocal of Kutateladze number for

experimental model with that of the present analytical model where different symbols are for a particular length-diameter combination of the heated tube. It is clear that the present model has the tendency to over-predict and under-predict the experimental CHF values. The analytical CHF values are as much as 50% higher than those of experimental values by Monde et al [3] for lower L_{he}/D while it is lower for higher L_{he}/D values. The possible reasons for these are explained briefly below.

For smaller L_{he}/D, the CHF characteristics is presumably similar to that of pool boiling giving its higher values as observed for both the present and existing experimental study. But the analytical values are much higher than the experimental values because here profile length, L is much higher than heated length, L_{he} for maximum mass flux. Thus the absence of the tube wall (Fig. 1) for z = 0 to (L – L_{he}) make some extra liquid to flow in into the main flow with less friction. The other reason is the lower value of 'n' as mentioned above. We must look for optimum value of 'n' that will improve our prediction.

(a)

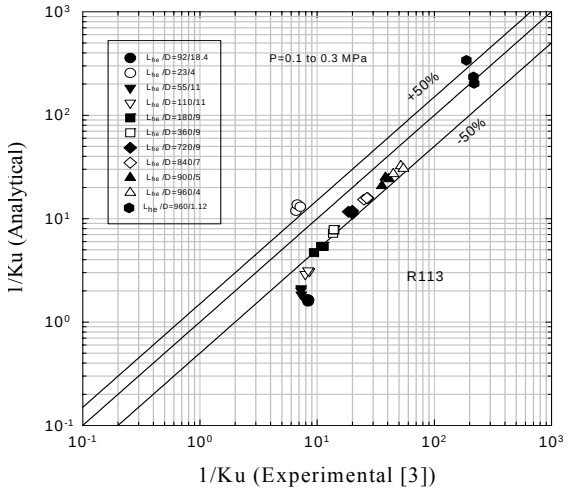

(b)

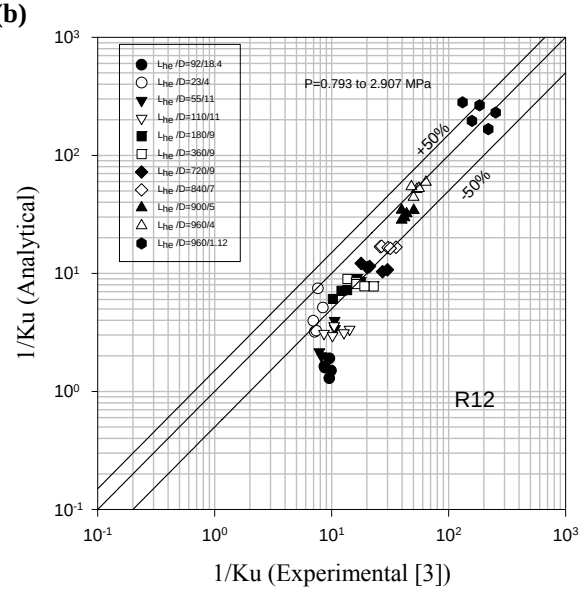

(c)

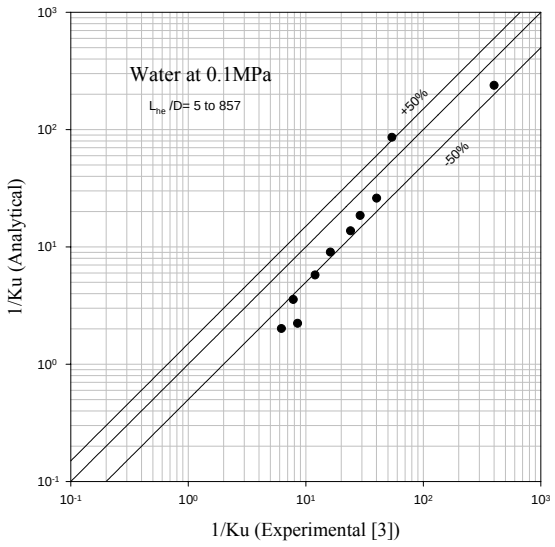

Fig 5. Performance of the present model

Again for $L_{he}/D>20$, the present analysis shows some discrepancies that are well above the +50% band as shown in Figs. 5(a-c). These may be attributed to the assumptions adopted in the present model. Acceleration of the vapor core during vaporization process very often produces entrainment of the liquid droplet. This effect, together with direct vaporization of the film, tends to reduce the film thickness quickly than with no entrainment resulting in the decrease in CHF. But the present model did not consider entrainment and thus over-predicts the CHF. Phase-change systems are almost always subjected to instability associated with the liquid-vapor interface. This kind of instability of interface has strong impact on heat and mass transfer during phase change process, which is not considered in the present model. This may also be one of the reasons of over-predicting CHF by this model.

4. CONCLUSIONS

(i) This model considers mass, momentum, and energy balances for the two-phase flow in a vertical tube submerged in a saturated liquid, where the liquid-vapor interface is a paraboloid formed by $z/L = (r/r_o)^n$ for $n \geq 2$. The CHF is assumed to be taken place at the exit of the heated tube when the void fraction is unity and the mass flux, G is maximum.

(ii) The predicted CHF values show the similar characteristics as shown in available experimental studies.

(iii) The variations of the CHF with L_{he}/D are more significant for $L_{he}/D<50$.

(iv) The liquid-vapor interface profile index, 'n' has significant effect on CHF upto value of 8 for R113, then further increase of its value shows very little effect on CHF.

(v) The predicted CHF agreed well with the experimental data within ±50% for $L_{he}/D> 20$.

5. REFERENCES

1. Y. Katto, 1978, "Generalized correlation for Critical Heat Flux of natural convection boiling in confined channels", Transaction of JSME (in Japanese), vol. 44, pp. 3908-3911.
2. Y. Katto and T. Kurosaka, 1979, "Critical Heat Flux of natural convection boiling in vertical annular channels", *Proceedings of the 15th National Heat Transfer Symposium of Japan,* pp. 280-282.
3. M. Monde and K. Yamaji, 1990, "Critical Heat Flux during natural convective boiling in vertical uniformly heated tubes submerged in saturated liquid", *Proceedings of 9th International Heat Transfer Conference,* Jerusalem, Israel, pp. 111-116.
4. M. Monde, S. Mihara, and T. Inoue, 1993, "An analytical study of the Critical Heat Flux of a Two-phase thermosiphon", Heat Transfer-Japanese Research, 22(6), pp. 611-623.
5. Y. Katto, and Yokoya, 1970, "Principal mechanism of boiling crisis in pool boiling", Intl. J. Heat and Mass Transfer 11, 993-1002.
6. Y. Haramura, and Y. Katto, 1983, "A new hydrodynamic model of Critical Heat Flux, applicable widely to both Pool and forced convection boiling on submerged bodies in saturated liquids", Int.l. J. Heat and Mass Transfer 26, 379-399.
7. P. B. Whalley, P. Hutchinson, and G. F. Hewitt, 1974, "The calculation of critical heat flux in forced convective boiling", *Proceedings of 5th Int. Heat Transfer Conf.,* Tokyo, Paper B6. 11.
8. P. B. Whalley, 1976, *The calculation of dryout in rod bundle*, Br. Report AERE-R8319.
9. P. B. Whalley, P. Hutchinson, and G. F. Hewitt,1974, *Prediction of annular flow parameters for transient flows and for complex geometries*, Br. Report AERE-M2661.
10. A. M. Govan, G. F. Hewitt, D. G. Owen, and T. R. Bott, 1988, "An improved CHF modeling code", *Proceedings of 2nd U.K. Conf. Heat Transfer,* Institute of Mechanical Engineers, London, vol. 1, pp. 33-48.
11. T. Okawa, A. Kotani, I. Katako, and M. Naito, 2003, "Prediction of Critical Heat Flux in annular flow using a film flow model", Journal of Nuclear Science and Technology, Vol. 40, N0. 6, pp. 388-396.
12. H. M. M. Afroz, 2004, "An analytical study of critical heat flux in natural convective boiling in a vertical tube," M.Sc. (ME) Thesis, BUET, pp. 21-31.
13. K. Stephan, 1987, *Heat transfer in condensation and boiling*, pp.160-161, Springer-Verlag.

6. NOMENCLATURE

Symbol	Meaning	Unit
A	Cross sectional area of tube	(m^2)
C_{fw}	Wall friction factor	(-)
D	Tube diameter	(m)
G	mass flux	(kg/m^2s)
g	Gravitational acceleration	(m/s^2)
H_{lg}	Latent heat of evaporation	(kJ/kg)
j_l	Superficial liquid velocity	(m/s)
Ku	Kutateladze number $= \frac{q_{co}/\rho_v H_{lg}}{\sqrt[4]{\sigma g(\rho_l-\rho_v)/\rho_v{}^2}}$	(-)
L	Liquid-vapor interface profile length	(m)
L_{he}	Tube heating length	(m)
L^+	$= L_{he}/L$	(-)
n	Profile index	(-)
P	System pressure	(MPa)
q_{co}	CHF for saturated boiling	(kW/m^2)
Re_l	Reynolds number for liquid	(-)
r	Radial coordinate	(m)
r_o	Radius of the tube	(m)
u	Fluid velocity	(m/s)
z	Vertical coordinate along the length of the tube	(m)
z^+	$= z/L$	(-)
ρ	Fluid Density	(kg/m^3)
σ	Surface tension	(N/m)
τ_i	Interfacial shear stress	(N/m^2)
τ	Shear stress	(N/m^2)
α	Void fraction $=A_v/A$	(-)
μ	Viscosity	(Pa.s)